A facile chemical approach for preparing a SERS active silver substrate†

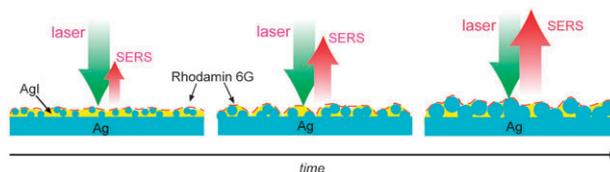Cheng Yang,‡*[a] Yu-Tao Xie,‡[b] Matthew M. F. Yuen,*[a] Xiaomin Xiong[c] and C. P. Wong*[d]

This communication describes a new surface-enhanced Raman scattering (SERS) active silver substrate prepared by iodination of the evaporated silver foil. After iodination, the morphology of the silver substrate undergoes a self-evolution process in which it displays accordingly the UV-vis absorption shift as well as the AFM topological test. Rhodamine 6G (R6G) is used as the probe molecule to evaluate the enhancement efficiency of the silver substrate at different self-evolution time intervals. The SERS intensity of R6G increases up to ∼29-fold and reaches a maximum after the substrate evolved for 24 h. This method is feasible for the production of an efficient SERS silver substrate.

Here we report a simple silver iodination method to generate a SERS active substrate on a sputtered silver foil. As silver is one of the best materials for preparing SERS active substrates (because its dielectric constant near the Frohlich frequency results in an intense surface plasmon resonance),[1] researchers have been searching for effective methods to develop SERS active silver substrates. To this end, many methods have been proposed, such as electrochemical oxidation/reduction methods,[2] vacuum evaporation deposition,[3] mirror reaction,[4] sputtering coating,[5] mechanical polishing with abrasives,[6] plasma treatment,[7] nanosphere lithography-E beam,[8] and laser ablation etc.[9] The resulting substrates gain a variety of structures containing the well distributed "hot spots", so that the weak basic Raman signals of the analytes can be effectively enhanced.[10] For all the methods, producing cost-effective and reproducible large-area SERS active substrate in simple steps remains a major challenge.

To the best of our knowledge, one of the simplest methods for fabricating large-area SERS active substrates may be directly treating the bulk noble metal or evaporated foil surface by solution processes. Here we adopt a solution-based iodination treatment to the evaporated silver foil surface and obtain a SERS active silver substrate. Silver iodide features a superionic conductivity property[11] and usefulness in cloud-seeding;[12] while there are very limited reports about using AgI as an active component to activate SERS activity of silver.[13] When the silver surface is being iodinated, the

diffusion-controlled inward movement of iodine at the silver surface may result in a layer of defect-abundant non-stoichiometric Ag/AgI structures,[14] the defects (e.g., vacancies) around the Ag/AgI boundary or space-charge regions gain enhancing effect with respect to the transport of mobile Ag^+ cations,[15] which subsequently lead to AgI decomposition at the silver surface and structural reconstructions, producing numerous fresh metallic silver clusters.[16] Here we first report our work by utilizing this strategy for SERS active substrate preparation and elucidate our study on the SERS activity vs. UV-vis optical absorption spectrum of the substrate at different time intervals. Since the iodination process can take place very homogeneously on a large area substrate, this features an extremely convenient and cost-effective pathway in the final design of parallel investigations of many SERS active substrates at the same time (Fig. 1).

The UV-vis absorption spectra provide the change of surface plasmon resonance of the silver substrate after iodination, based on which, it is indicative of the optimum SERS substrate. The UV-vis absorption of silver nano-materials is highly dependent on the particle size, morphology, geometric structures and the surrounding dielectric environment. As displayed in Fig. 2, the freshly iodinated silver foil sample shows a broad absorption band at ∼370 nm and the other distinct sharp absorption at ∼427 nm. The former gets dominant as time elapses, which is assignable to the surface plasma resonance of the Ag^0_n clusters;[17] while the latter is assigned to the characteristic band of β-AgI (wurtzite), induced by the forbidden transition ($4d^{10}$ to $4d^9 5s^1$) in the Ag ion which becomes allowed due to the tetrahedral symmetry of the Ag ion site.[18] As time passes by, the UV-vis absorption varies in both the band position and the relative absorption intensity. The absorption band at ∼370 nm gets stronger and dominant, while the band at ∼427 nm becomes broader and relatively weak in intensity, accompanying a pretty broad absorption band centered at ∼600 nm after three hours. This absorption band is induced by the plasmon coupling in a long range or a high-order coupling effect of a multi-Ag-particle. The related surface morphology is displayed in Fig. 3b for the sample after 3 h. Though the mechanism is not clearly understood, this phenomenon indicates that the nanoparticle (Ag or AgI, or both) has a

[a] Department of Mechanical Engineering, The Hong Kong University of Science and Technology, Clear Water Bay, Hong Kong, China. E-mail: yangch@ust.hk, meymf@ust.hk; Fax: +852 23581543; Tel: +852 23588814
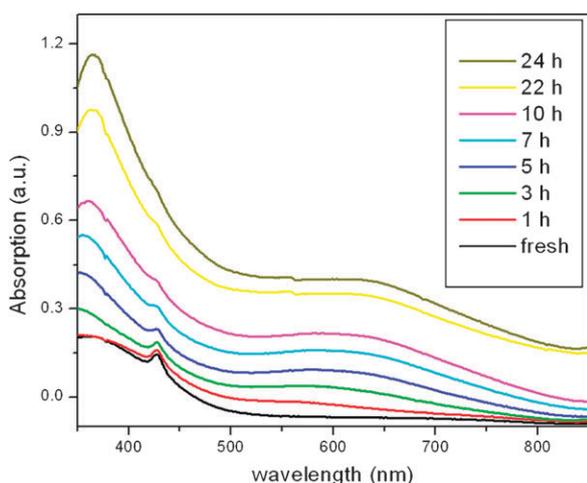[b] Department of Chemistry, The Hong Kong University of Science and Technology, Clear Water Bay, Hong Kong, China
[c] Department of Physics, Sun Yet-sen University, Guangzhou, China
[d] School of Materials and Engineering, Georgia Institute of Technology, Atlanta, GA, USA. E-mail: cp.wong@mse.gatech.edu; Fax: +1 4048949140; Tel: +1 4048948391
† Electronic supplementary information (ESI) available: Sample preparation and Raman measurement. See DOI: 10.1039/c0cp00414f
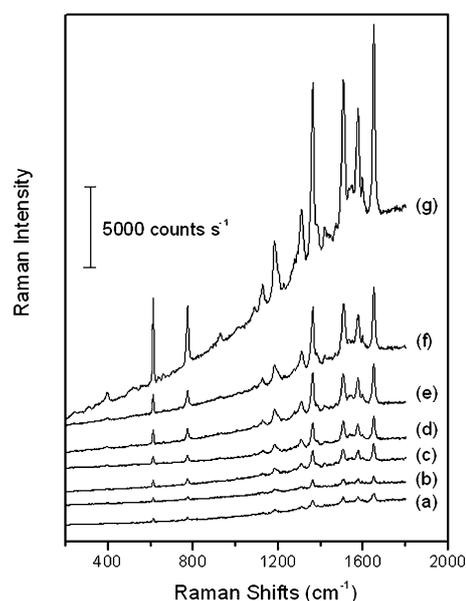‡ Equal contribution.

Fig. 1 A schematic of the increase of SERS activity of the iodinated silver foil surface with time.

This journal is © the Owner Societies 2010

Phys. Chem. Chem. Phys., 2010, **12**, 14459–14461 | 14459

Fig. 2 UV-vis absorption spectra (reflective mode) of the iodinated silver evaporated wafer surface at different time intervals after the iodination treatment.

Fig. 4 SERS spectra of the R6G on the iodinated silver evaporated wafer surface at different time intervals after the iodination treatment: (a) 20 min after the treatment; (b) 90 min after the treatment; (c) 140 min after the treatment; (d) 4.5 h after the treatment; (e) 6.5 h after the treatment; (f) 16 h after the treatment; (g) 24 h after the treatment (the reference bar shows the Raman intensity of 5000 counts s^{-1}).

more inhomogeneous distribution in particle size. This evolution reaches a steady state after 24 h. When the particle size increases, higher order surface modes may become dominant, which may induce a shift of the absorption maximum toward lower energies, a broadening of the absorption band.[19] Fig. 3 shows the morphology of the silver sample after the iodination treatment in a 24-hour time series. The bump-shaped silver nanostructure forms and grows as time passes by. After 24 h, the size of all the nanostructures gets to a similar shape with the size of ∼300 nm and height of ∼70 nm. The corresponding optical property of this surface morphology is a broad adsorption band at ∼600 nm in the UV-vis absorption spectrum in Fig. 2.

Fig. 4 displays the SERS spectra of Rhodamine 6G (R6G) on the iodinated silver samples at different time intervals. The spectrum is dominated by the peaks at 1651, 1576, 1512, 1365, 1312, 775, and 614 cm^{-1}, of which the assignments have been well documented in the literature.[20] The result suggests that R6G molecules might contact the substrate through xanthene

groups and probably in end-on configuration. It can be clearly seen that it shows most strong SERS intensity for the silver substrate after 24 h. In order to better view the high efficient SERS performance of silver substrate after 24 h, the intensity ratio (I_t/I_{fresh}) is calculated: $I_{t-6\,h}/I_{fresh} = 6$; $I_{t-16\,h}/I_{fresh} = 9.5$; $I_{t-24\,h}/I_{fresh} = 28.5$.

The main origin of the efficient Raman enhancement from the silver substrate in this communication results from the subsequent surface plasmon change induced by the morphology evolution of the Ag particles after iodination treatment. The final particle size created by the iodination process is ∼300 nm (Fig. 3d) and therefore is highly suitable for a SERS
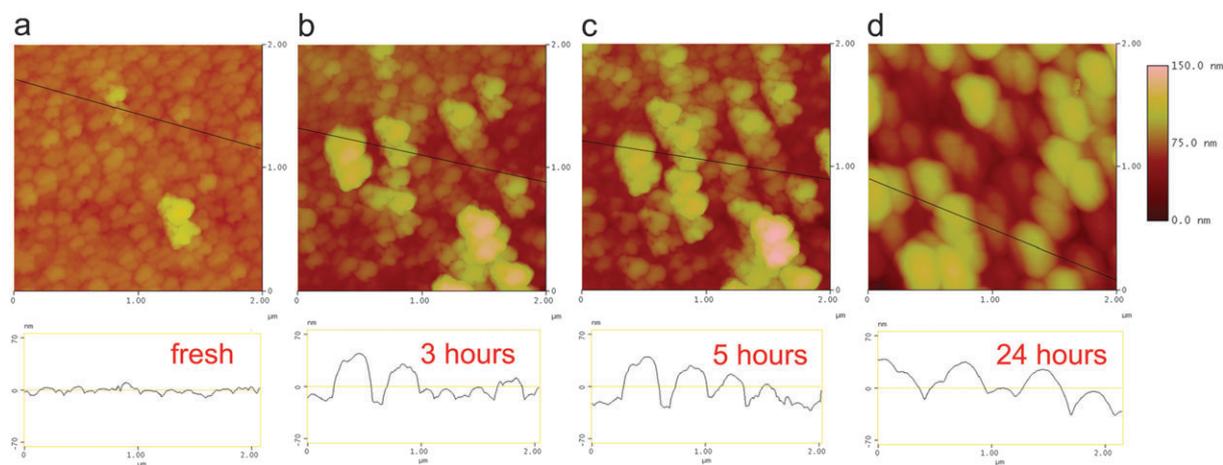
Fig. 3 AFM topology of the iodinated silver evaporated wafer surface at different time intervals after the iodination treatment: (a) freshly prepared; (b) 3 h after the treatment; (c) 5 h after the treatment; (d) 24 h after the treatment. A partition line is drawn in each image to show the height profile of the sample (below each image), demonstrating the variation of height in the same region.

active substrate, which agrees very well with the report by Nie *et al.* that the optimum particle size providing the greatest SERS enhancement in the wavelength region around 500 nm, was of the order of 100 nm in diameter or even higher.[21] On the other hand, localized surface plasmon resonance modes created by strong electromagnetic coupling between touching metallic particles are known to play a key role in surface enhancement.[22] Brus *et al.* showed that a particularly strong SERS enhancement was created between two metal colloids, as so-called "hot spot".[23] Comparing the four AFM images in Fig. 2, it is found that collections of silver nanoparticles are formed on the silver surface after 24 h. This morphology can generate a high number of hot spots for Raman enhancement, which is consistent with both the related shifts of UV-vis absorption and the maximum SERS intensity in Fig. 3.

In summary, we present here a simple iodination method to form a SERS active substrate, which exhibits analogous absolute Raman signal intensity of R6G to that reported elsewhere in the literature,[20] which may be on more complicated and expensive substrates. The SERS intensity of R6G increases up to ∼29-fold and reaches a maximum after the substrate evolved for 24 h. Our approach presents several advantages: first, the process is very simple and convenient for preparing very large areas compared to conventional ones; second, it is instructive for investigations of the relationship between the Localized Surface Plasmon Resonance (LSPR) of the substrate and the best SERS signals and further to optimize the effective SERS substrate; finally, the method is very reproducible and the hot spot is homogeneously distributed in the AgI dielectric environment at the substrate surface for the attachment of analytes. This method provides a simple way to fabricate highly effective SERS substrates without the limitation of substrate dimension. Considering the simplicity, convenience, and low cost for fabricating large SERS-active surfaces on silver foils, we envisage various applications of this simple technique in large in-the-field or parallel diagnosis.

Acknowledgements

References

1 M. Moskovits, *J. Raman Spectrosc.*, 2005, **36**, 485–496.
2 A. Gutés, C. Carraro and R. Maboudian, *J. Am. Chem. Soc.*, 2010, **132**, 1476–1477.
3 H. Yamada and Y. Yamamoto, *Surf. Sci.*, 1983, **134**, 71–90.
4 Y. Saito, J. J. Wang, D. N. Batchelder and D. A. Smith, *Langmuir*, 2003, **19**, 6857–6861.
5 K. Bandyopadhyay, K. Vijayamohanan, M. Venkataramanan and T. Pradeep, *Langmuir*, 1999, **15**, 5314–5322; C. H. Xu, X. Chen, Y. J. Liu, B. Xie, M. Han, F. Q. Song and G. H. Wang, *Nanotechnology*, 2010, **21**, 6.
6 M. Baibarac, L. Mihut, G. Louarn, J. Y. Mevellec, J. Wery, S. Lefrant and I. Baltog, *J. Raman Spectrosc.*, 1999, **30**, 1105–1113.
7 M. Rosenberg, D. P. Sheehan and J. R. Petrie, *J. Phys. Chem. A*, 2004, **108**, 5573–5575.
8 J. C. Love, L. A. Estroff, J. K. Kriebel, R. G. Nuzzo and G. M. Whitesides, *Chem. Rev.*, 2005, **105**, 1103–1169; C. L. Haynes and R. P. Van Duyne, *J. Phys. Chem. B*, 2001, **105**, 5599–5611.
9 C. D. Geddes, A. Parfenov, D. Roll, J. Y. Fang and J. R. Lakowicz, *Langmuir*, 2003, **19**, 6236–6241.
10 Y. C. Liu and T. C. Chuang, *J. Phys. Chem. B*, 2003, **107**, 9802–9807; J. E. Pemberton, A. L. Guy, R. L. Sobocinski, D. D. Tuschel and N. A. Cross, *Appl. Surf. Sci.*, 1988, **32**, 33–56; S. A. Maier, in *Plasmonics: Fundamentals and Applications*, Springer, Bath, 2007, pp. 165–169.
11 S. Hull, *Rep. Prog. Phys.*, 2004, **67**, 1233–1314.
12 L. J. Battan, *J. Appl. Meteorol.*, 1967, **6**, 317–322.
13 X. L. Li, Y. F. Wang, H. Y. Jia, W. Song and B. Zhao, *J. Raman Spectrosc.*, 2005, **36**, 635–639; X. L. Li, W. Q. Xu, J. H. Zhang, H. Y. Jia, B. Yang, B. Zhao, B. F. Li and Y. Ozaki, *Langmuir*, 2004, **20**, 1298–1304.
14 P. Senthil Kumar and C. S. Sunadana, *Proc. SPIE*, 2002, **4807**, 241–252.
15 J. S. Lee, S. Adams and J. Maier, *J. Phys. Chem. Solids*, 2000, **61**, 1607–1622; L. M. Slifkin, *Cryst. Lattice Defects Amorphous Mater.*, 1989, **18**, 81–96.
16 K. Matsunaga, I. Tanaka and H. Adachi, *J. Phys. Soc. Jpn.*, 1998, **67**, 2027–2036.
17 K. Shimizu, J. Shibata, H. Yoshida, A. Satsuma and T. Hattori, *Appl. Catal., B*, 2001, **30**, 151–162; C. Hu, T. W. Peng, X. X. Hu, Y. L. Nie, X. F. Zhou, J. H. Qu and H. He, *J. Am. Chem. Soc.*, 2010, **132**, 857–862; F. Q. Song, T. Y. Wang, X. F. Wang, C. H. Xu, L. B. He, J. G. Wan, C. Van Haesendonck, S. P. Ringer, M. Han, Z. W. Liu and G. H. Wang, *Small*, 2010, **6**, 446–451.
18 D. B. Mohan, K. Sreejith and C. S. Sunandana, *Appl. Phys. B: Lasers Opt.*, 2007, **89**, 59–63; D. B. Mohan and C. S. Sunandana, *J. Appl. Phys.*, 2006, **100**, 10; S. Frederick, *Rev. Mod. Phys.*, 1951, **23**, 328–352; S. Tutihasi, *Phys. Rev.*, 1957, **105**, 882–884; J. Belloni, *Radiat. Phys. Chem.*, 2003, **67**, 291–296.
19 C. F. Bohren and D. R. Hoffman, *Absorption and Scattering of Light by Small Particles*, Wiley, 1983.
20 P. Hildebrandt and M. Stockburger, *J. Phys. Chem.*, 1984, **88**, 5935–5944.
21 S. M. Nie and S. R. Emery, *Science*, 1997, **275**, 1102–1106.
22 F. J. GarciaVidal and J. B. Pendry, *Phys. Rev. Lett.*, 1996, **77**, 1163–1166.
23 A. M. Michaels, J. Jiang and L. Brus, *J. Phys. Chem. B*, 2000, **104**, 11965–11971; J. I. Gersten and A. Nitzan, *Surf. Sci.*, 1985, **158**, 165–189.